Journal of Bacteriology

Deletion of the Desulfovibrio vulgaris Carbon Monoxide Sensor Invokes Global Changes in Transcription

Lara Rajeev, Kristina L. Hillesland, Grant M. Zane, Aifen Zhou, Marcin P. Joachimiak, Zhili He, Jizhong Zhou, Adam P. Arkin, Judy D. Wall and David A. Stahl

J. Bacteriol. **2012, 194(21):5783. DOI: 10.1128/JB.00749-12. Published Ahead of Print 17 August 2012.**

JB
Journals.ASM.org

Deletion of the *Desulfovibrio vulgaris* Carbon Monoxide Sensor Invokes Global Changes in Transcription

Lara Rajeev,[a]* Kristina L. Hillesland,[a,c] Grant M. Zane,[d] Aifen Zhou,[e] Marcin P. Joachimiak,[b] Zhili He,[e] Jizhong Zhou,[e] Adam P. Arkin,[b] Judy D. Wall,[d] and David A. Stahl[a]

Department of Civil and Environmental Engineering, University of Washington, Seattle, Washington, USA[a]; Physical Biosciences Division, Lawrence Berkeley National Laboratory, Berkeley, California, USA[b]; Science and Technology Program, University of Washington, Bothell, Washington, USA[c]; Department of Biochemistry, University of Missouri, Columbia, Missouri, USA[d]; and Institute of Environmental Genomics, Department of Microbiology and Plant Biology, University of Oklahoma, Norman, Oklahoma, USA[e]

The carbon monoxide-sensing transcriptional factor CooA has been studied only in hydrogenogenic organisms that can grow using CO as the sole source of energy. Homologs for the canonical CO oxidation system, including CooA, CO dehydrogenase (CODH), and a CO-dependent Coo hydrogenase, are present in the sulfate-reducing bacterium *Desulfovibrio vulgaris*, although it grows only poorly on CO. We show that *D. vulgaris* Hildenborough has an active CO dehydrogenase capable of consuming exogenous CO and that the expression of the CO dehydrogenase, but not that of a gene annotated as encoding a Coo hydrogenase, is dependent on both CO and CooA. Carbon monoxide did not act as a general metabolic inhibitor, since growth of a strain deleted for *cooA* was inhibited by CO on lactate-sulfate but not pyruvate-sulfate. While the deletion strain did not accumulate CO in excess, as would have been expected if CooA were important in the cycling of CO as a metabolic intermediate, global transcriptional analyses suggested that CooA and CODH are used during normal metabolism.

Desulfovibrio organisms are sulfate-reducing bacteria that use organic acids, alcohols, or molecular hydrogen as electron donors to reduce sulfate (22). When these bacteria grow on organic acids or alcohols, energy generation is hypothesized to be derived in part through hydrogen cycling (20). Hydrogen cycling posits that reducing equivalents formed during oxidation of the electron donor in the cytoplasm are shuttled to form hydrogen, which is then oxidized in the periplasm to generate electrons for sulfate reduction and to generate a proton motive force. This mechanism for energy recovery offers an explanation for the hydrogen burst observed during the early growth phase in batch culture (15, 19, 20, 28). *Desulfovibrio vulgaris* Hildenborough appears well equipped to carry out this hydrogen cycling, possessing an array of six predicted hydrogenases—four localized periplasmically (Hyd, Hyn1, Hyn2, and Hys) and two membrane-bound enzymes facing the cytoplasm (Coo and Ech) (12). There is also some evidence suggesting that, in addition to hydrogen, carbon monoxide functions as either a growth substrate or an intermediate in energy metabolism (16, 29).

With the exception of some *Desulfotomaculum* species that can grow in >50% CO, CO is toxic at concentrations of <20% to most sulfate-reducing bacteria (21). CO toxicity is likely to be a result of inhibition of hydrogenases or other metalloenzymes (21). CO has been demonstrated to be both produced and consumed by *Desulfovibrio* spp. CO production has been documented during growth of both *D. vulgaris* Hildenborough (29) and *D. vulgaris* Madison (16) on lactate-sulfate or pyruvate-sulfate, with greater accumulation in a *D. vulgaris* Hildenborough *hyd* mutant lacking the periplasmic Fe hydrogenase (29). Consumption was demonstrated in *D. vulgaris* strain Madison. This organism grew on a headspace of 4% CO as the sole energy source and tolerated a headspace of 4.5% CO while growing on organic acids, consistent with the presence of an active CO dehydrogenase (CODH) (16). In turn, a gene predicted to code for a monofunctional CODH (*cooS*) was identified in the genome sequence of *D. vulgaris* Hildenborough and is similar to the *cooS* genes from CO-utilizing hydrogenogenic organisms such as *Rhodospirillum rubrum* and *Carboxydothermus hydrogenoformans* (14, 31).

R. rubrum and *C. hydrogenoformans* grow anaerobically on CO as the sole energy source by evolving H_2 (Fig. 1). Their carbon monoxide oxidation (*coo*) system consists of two operons: *cooFSCTJ*, encoding CODH, and *cooMKLXUH*, encoding a CO-dependent hydrogenase (Fig. 1) (9, 14). These operons are regulated by the *cooA* gene, encoding a CO-sensing transcriptional activator (11, 25). The best-studied CooA, that of *R. rubrum* (a facultative aerobe), is a homodimeric heme-containing protein that acts both as a specific CO sensor and as a redox sensor (13), with only the reduced form of the CooA heme able to bind CO.

In this study, we sought to understand in greater depth the CO metabolism of *D. vulgaris* Hildenborough, since this strain benefits from a completed genome sequence (12) and a genetic system. Although a CO sensor has not been described so far for a sulfate-reducing bacterium, *D. vulgaris* Hildenborough carries a gene, annotated *cooA*, that lies upstream of the CODH operon (*cooSC*). The *cooA* gene and the associated *cooSC* genes are conserved in several *Desulfovibrio* species and other closely related sulfate reducers, suggesting that CooA has an important role in the physiology of these bacteria. Additionally, *D. vulgaris* Hildenborough has a *cooMKLXUHF* hydrogenase operon elsewhere in the genome that is homologous to the CO-dependent Coo hydrogenase

Received 4 May 2012 **Accepted** 13 August 2012
Published ahead of print 17 August 2012
Address correspondence to Lara Rajeev, lrajeev@lbl.gov.
* Present address: Lara Rajeev, Physical Biosciences Division, Lawrence Berkeley National Laboratory, Berkeley, California, USA.

doi:10.1128/JB.00749-12

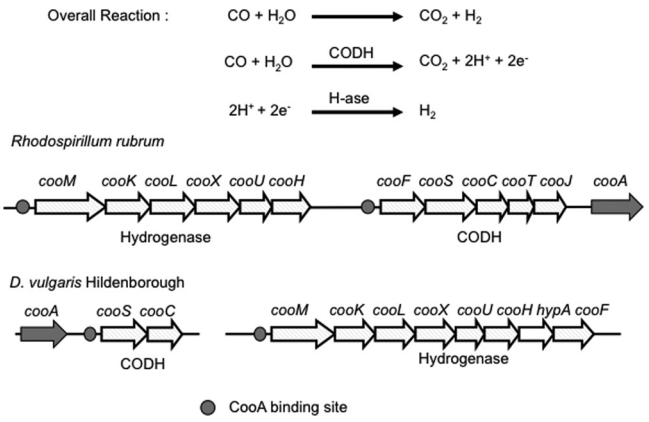

FIG 1 *coo* operons of *Rhodospirillum rubrum* and *Desulfovibrio vulgaris* Hildenborough. CO is oxidized by CODH, and the reaction is coupled to hydrogen generation by a CO-dependent hydrogenase. *R. rubrum* carries the *cooMKLXUH* hydrogenase operon and the *cooFSCTJ* CODH operon adjacent to each other, with the regulatory *cooA* gene located downstream. The *D. vulgaris* genome has a *cooSC* CODH operon, with the *cooA* gene located upstream, but the *cooMKLXUHF* hydrogenase operon lies elsewhere in the chromosome. The filled circles represent the CooA binding sites (predicted sites for *D. vulgaris*) upstream of the hydrogenase and CODH operons.

operon of *R. rubrum* and *C. hydrogenoformans* but is not conserved among *Desulfovibrio* species. Binding sites for *D. vulgaris* CooA have been predicted in the upstream regions of the *cooSC* and *cooMKLUXHF* operons (23). Recently, the *D. vulgaris* Coo hydrogenase was identified as a major hydrogen-evolving hydrogenase that is essential for syntrophic growth with *Methanococcus maripaludis* on lactate (30). These observations led to the intriguing question of whether this important Coo hydrogenase is regulated by CO and/or CooA.

Here we show that *D. vulgaris* Hildenborough carries a functional CO dehydrogenase whose expression is dependent upon the presence of CO and the *cooA* gene. CooA is necessary for CO consumption by *D. vulgaris* and thus acts as a CO sensor. Unlike that seen for the hydrogenogenic organisms, Coo hydrogenase expression is independent of CO or CooA. We also implicate CooA in additional physiological roles by using culture headspace chemical characterization and genome-wide expression analysis.

MATERIALS AND METHODS

Strain growth. *Desulfovibrio vulgaris* Hildenborough was grown anaerobically on CCMA medium, pH 7.2, at 37°C, under a headspace of 20% CO_2-80% N_2. CCMA medium contained (per liter) 2.28 g NaCl, 5.5 g $MgCl_2 \cdot 6H_2O$, 0.14 g $CaCl_2 \cdot 2H_2O$, 1.0 g NH_4Cl, 0.1 g KCl, 30 mM sulfate, 25 mM $NaHCO_3$, 1.1 mM K_2HPO_4, 0.001 g resazurine, 1 mM $Na_2S \cdot 9H_2O$, 1 mM cysteine, 1 ml of Thauer's vitamins (containing [per liter] 0.02 g biotin, 0.02 g folic acid, 0.1 g pyridoxine HCl, 0.05 g thiamine HCl, 0.05 g riboflavin, 0.05 g nicotinic acid, 0.05 g DL-pantothenic acid, 0.05 g *p*-aminobenzoic acid, and 0.01 g vitamin B_{12}), and 1 ml of trace minerals (containing [per liter] 12.8 g of nitrilotriacetic acid, pH 6.5, 1.0 g $FeCl_2 \cdot 4H_2O$, 0.5 g $MnCl_2 \cdot 4H_2O$, 0.3 g $CoCl_2 \cdot 4H_2O$, 0.2 g $ZnCl_2$, 0.05 g $Na_2MoO_4 \cdot 4H_2O$, 0.02 g H_3BO_3, 0.1 g $NiSO_4 \cdot 6H_2O$, 0.002 g $CuCl_2 \cdot 2H_2O$, 0.006 g $Na_2SeO_3 \cdot 5H_2O$, and 0.008 g $Na_2WO_4 \cdot 2H_2O$), supplemented with either lactate (LS) or pyruvate (PS) (30 mM). Where indicated, carbon monoxide was added from a mixture of 50% CO-50% N_2 to achieve the desired headspace concentration. Cells were grown in either 25-ml Balch tubes with 10 ml medium or 250-ml serum bottles with 100 ml medium. Cultures with CO in the headspace were grown with shaking. Growth assays were initiated with a 2% inoculum from a late-exponential-phase culture. Growth measurements for Balch tube cultures were performed by measuring cell densities directly in the Balch tubes with a Hach spectrophotometer (Hach, Loveland, CO) at 600 nm. For bottle cultures, 1-ml cell samples were withdrawn, and the optical density at 600 nm (OD_{600}) was measured using a 1-mm-path-length cuvette.

Headspace gas measurements. The headspace hydrogen and carbon monoxide concentrations were measured by injecting 0.1 ml of sample into a Trace Analytical RGD2 reduction gas detector (Ametek, Newark, DE) equipped with a 60/80 Mole Sieve 5A column (72 1/8 in.), with N_2 as the carrier gas. For growth in the presence of CO, headspace samples were diluted 10- to 100-fold in a stoppered serum vial that was flushed with nitrogen gas prior to injection into the column.

Sulfide determination. Dissolved sulfide in culture medium was determined by the method of Cord-Ruwisch (5), using 0.1 ml of culture and 4 ml of $CuSO_4$-HCl reagent. Absorbance was measured at 480 nm, and sulfide concentrations were determined using a standard curve prepared with dilutions of anoxic sodium sulfide solution.

Growth on CO as the sole energy source. A 10% inoculum of a culture grown on PS plus 2% CO was added to Balch tubes containing 10 ml CCMA medium supplemented with 5 mM acetate and 30 mM sulfate and with a headspace of 80% N_2-20% CO_2. CO (from 50% CO-50% N_2) was added to the tubes in small increments, as follows. For the wild type (WT), 0.7 ml was added on days 0 and 4, 1 ml on days 5 and 7, 1.2 ml on day 10, and 1.5 ml on days 13, 15, 19, and 20; on day 21, the three replicates received 1.5, 2.0, and 2.5 ml. For strain JW3034 (*cooL* mutant) (30), 0.7 ml was added on day 0, 1 ml on days 5, 8, 10, and 14, 1.2 ml on days 15 and 16, and 1.5 ml on day 19. The *cooA* mutant (strain JW9009) received 0.7 ml CO on day 0. Headspace CO was measured by analyzing a 1:100 dilution of the headspace sample by use of the RGD gas detector (see above). When CO was less than 1% of the starting amount, the next addition of CO was made.

Construction of Δ*cooA* mutant JW9009. Construction of the *cooA* (DVU2097) deletion strain was similar to that previously described (33). In short, three regions were PCR amplified: a 900-bp region upstream of the *cooA* start codon, 948 bp downstream of the *cooA* stop codon, and a kanamycin resistance marker. The three PCR products were combined together in a fourth PCR mix with the outermost primers for an overlap extension PCR. The product was cleaned, captured in the pCR8/GW/TOPO vector (Invitrogen, Carlsbad, CA), sequenced, and named pMO9008. Plasmid pMO9008 (775 ng) was electroporated (1,750 V, 250 Ω, 25 μF) into *D. vulgaris* Hildenborough as described previously (33). Transformants selected for resistance to G418, a kanamycin analogue, were then screened for sensitivity to spectinomycin (100 mg/ml), which was expected for a marker exchange by double homologous recombination. A Southern blot confirmed deletion of the *cooA* gene, and one isolate was designated JW9009.

Complementation of *cooA*. The *cooA* gene and 270 bp upstream was PCR amplified, cloned by restriction digestion into the *Escherichia coli-D. vulgaris* shuttle vector pMO719, transformed into *E. coli*, and selected for spectinomycin-resistant clones. The resulting plasmid was isolated from the transformants and sequenced to verify the presence of the insert. The positive plasmid construct was electroporated into JW9009 cells as described previously (33), and transformants were selected for resistance to spectinomycin. Colony PCR and sequencing were used to confirm the presence of the *cooA* gene in JW9009, and the complemented strain was named JW9009(pMO719::*cooA*).

Reverse transcription-PCR (RT-PCR) analysis. Strains were grown in 100-ml bottles with 50 ml CCMA medium supplemented with 30 mM lactate. The wild-type, JW9009, and JW9009(pMO719::*cooA*) strains were inoculated (2% inoculum) into 2 bottles each from late-log-phase cultures and incubated without shaking. At an OD_{600} of 0.1, one bottle for each strain was harvested, while 0.5 ml of CO was added to the second bottle and incubated with shaking. After 1 h of exposure to CO, the second bottle was also harvested. Total RNA was prepared using a MasterPure RNA purification kit (Epicentre Biotechnologies, Madison, WI). The

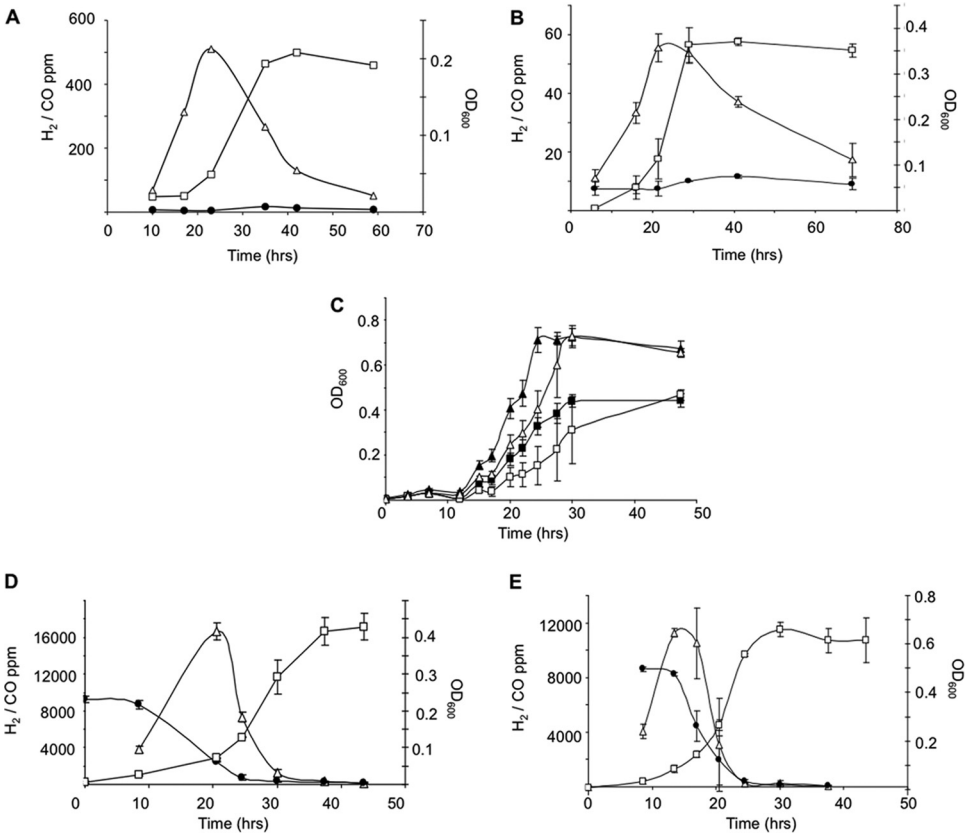

FIG 2 Wild-type *D. vulgaris* Hildenborough has an active CO dehydrogenase. Growth (open squares), hydrogen (open triangles), and CO (closed circles) profiles for the wild type on LS (A), PS (B), LS plus 1% CO (D), and PS plus 1% CO (E). (C) Growth curves for the wild type on LS (closed squares), LS plus 1% CO (open squares), PS (closed triangles), and PS plus 1% CO (open triangles). Data for panels A and B are for growth in 250-ml bottles with 100 ml medium, with OD_{600} readings taken by withdrawing 1-ml aliquots into cuvettes. Data for panels C, D, and E are for growth in 25-ml Balch tubes with 10 ml medium, with OD_{600} readings measured directly in the Balch tubes, hence resulting in higher values than those of the cuvette readings. The data are averages for 2 to 4 replicates, and error bars represent standard deviations for *n* values of >2.

RNA was reverse transcribed using an Ambion Retroscript first-strand synthesis kit (Life Technologies, Carlsbad, CA), and 5-fold serial dilutions of the cDNA were used as templates to PCR amplify the *cooS*, *cooL*, and *rpoH* transcripts.

Transcriptomic analysis. The wild-type and JW9009 strains were grown in a pyruvate-sulfate medium in the presence and absence of CO in the headspace, to an OD_{600} of 0.3. The cells were harvested, and total cellular RNA and genomic DNA (gDNA) isolation and purification were carried out as described previously (4). cDNA was labeled with Cy5-dUTP through reverse transcription with 10 μg of total RNA and random primers (27). Genomic DNA was labeled with Cy3-dUTP by use of random primers and the Klenow fragment as previously described (27). Labeled cDNA and gDNA were dried and stored at −20°C before hybridization. A *D. vulgaris* whole-genome oligonucleotide (70-mer) microarray covering 3,482 of the 3,531 protein-encoding sequences of the *D. vulgaris* genome (10) was used in this study. Array hybridizations were performed as described previously (34). Briefly, Cy5-labeled cDNA from each sample was cohybridized with Cy3-labeled gDNA (as a control for normalization across samples) on a microarray slide (Tecan HS4800; Tecan Group Ltd., Durham, NC). After a 10-h hybridization at 45°C with 50% (vol/vol) formamide, the microarray slides were dried and scanned for fluorescence intensity (ScanArray Express microarray analysis system; Perkin Elmer, Boston, MA). The data processing was done as described previously (17).

Microarray data accession number. The array data have been deposited in NCBI's Gene Expression Omnibus under GEO accession no. GSE36770.

RESULTS

***D. vulgaris* Hildenborough has an active CO dehydrogenase.** The wild-type *D. vulgaris* Hildenborough strain produced trace amounts of CO during growth on lactate-sulfate (LS) and pyruvate-sulfate (PS) (Fig. 2A and B). To assess the possible function of the annotated *cooS* gene of *D. vulgaris* Hildenborough as a CO dehydrogenase, we first grew the strain on lactate-sulfate or pyruvate-sulfate with 1% CO in the headspace. CO did not affect the final yield of the wild-type strain on either medium, although the growth was slower in the presence of CO (Fig. 2C). An analysis of the headspace showed that the CO was consumed on both LS and PS (Fig. 2D and E) and that a very pronounced hydrogen burst occurred in the presence of CO.

Strain JW9009 (Δ*cooA*) does not consume exogenous CO. Using a double-recombination strategy, we replaced the *cooA* gene (DVU2097) in the chromosome with a kanamycin resistance marker (see Materials and Methods) to generate strain JW9009. Under a headspace of 1% CO, the growth of strain JW9009 on lactate-sulfate was very slow compared to that of the wild type and reached an OD_{600} of 0.2 after 100 h (Fig. 3A). In contrast, the growth on pyruvate-sulfate with 1% CO was affected only slightly (Fig. 3B). Analysis of the headspace showed that the *cooA* mutant was unable to consume CO (Fig. 3C and D) on either LS or PS. On

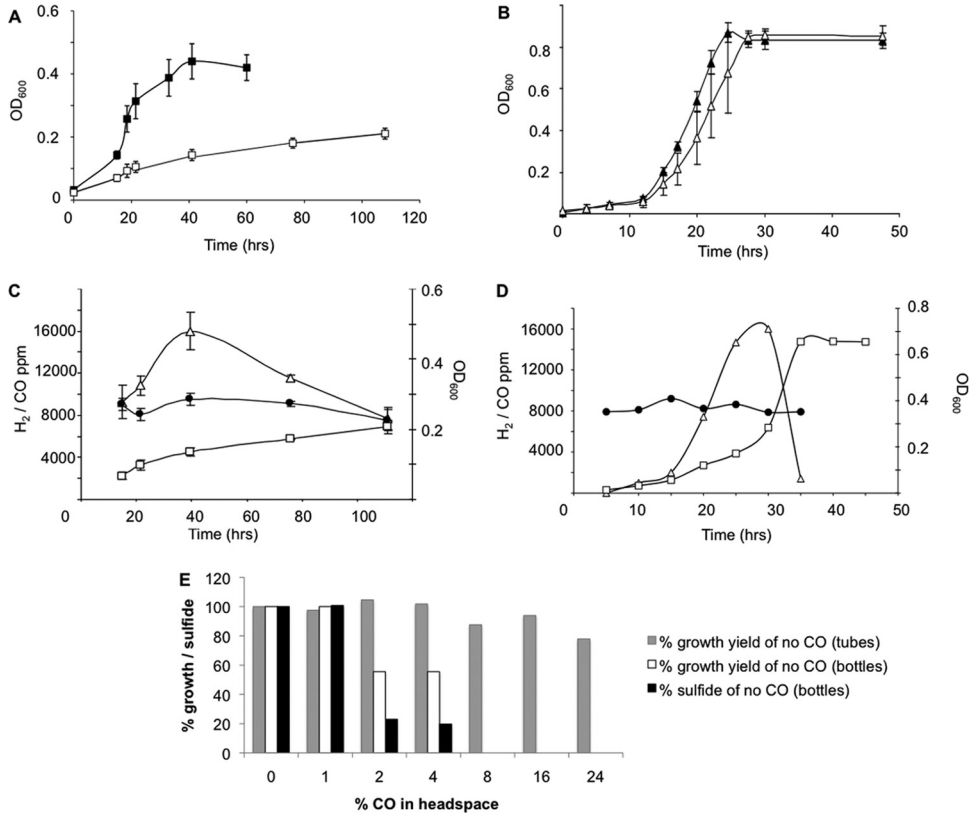

FIG 3 JW9009 does not consume CO. (A) Growth of JW9009 on LS (closed squares) and LS plus 1% CO (open squares). (B) Growth of JW9009 on PS (closed triangles) and PS plus 1% CO (open triangles). (C and D) Growth (open squares), CO consumption (closed circles), and H_2 (open triangles) profiles during growth on LS plus 1% CO (C) and PS plus 1% CO (D). Data for panels A to D are for growth in 25-ml Balch tubes with 10 ml medium, with OD_{600} readings measured directly in the Balch tubes. The data are averages for 2 to 4 replicates, and error bars represent standard deviations for *n* values of >2. (E) Growth yields (maximum OD_{600}) and dissolved sulfide production for JW9009 on PS with increasing amounts of CO in the headspace, presented as percentages of growth and sulfide in the absence of CO. For each increment in the % headspace CO, cultures from the previous CO tubes were used as the inoculum. Growth in tubes refers to 25-ml Balch tubes with 10 ml medium, as for panels A to D, and % yield was calculated using average OD_{600} readings for 4 replicates. Growth in bottles refers to 125-ml bottles with 50 ml medium, with OD_{600} readings measured by withdrawing aliquots into a cuvette and % yield and sulfide calculated using averages for two replicates.

PS, a large hydrogen burst was similar to that of the wild type, and the hydrogen was consumed at the end of growth even though the CO was not removed. On LS, the hydrogen that accumulated was removed by the mutant at a much lower rate than that seen for the wild type. The difference in sensitivity to CO between growth on lactate and that on pyruvate was more pronounced when JW9009 was exposed to higher concentrations of CO. On PS, we observed growth with as high as 24% CO, with a drop in the maximum cell densities seen only with CO concentrations of >8% ($P < 0.05$) (Fig. 3E). Since the lag time for growth was very long when the cells were inoculated directly into media with high headspace CO concentrations, cells exposed to lower CO levels were used to inoculate tubes with higher CO concentrations. The sensitivity of the cells was greater when the cells were grown in bottles (with the same headspace-to-medium volume ratio, but shaken on the side to allow for more surface area exposed to CO), with growth yields decreasing with as little as 2% CO (Fig. 3E) and growth occurring with longer lag times (not shown). Measurements of dissolved sulfide indicated that at concentrations of 2% CO and higher, JW9009 was fermenting and not respiring pyruvate (Fig. 3E). The expected maximum yield of sulfide for growth on 30 mM pyruvate is 7.5 mM sulfide, and we detected approximately 3.75 mM dissolved sulfide in WT and JW9009 cultures without CO.

***D. vulgaris* Hildenborough shows poor growth on CO as the sole energy source.** We then tested if *D. vulgaris* Hildenborough could grow by utilizing CO as the sole energy source on medium supplemented with acetate in a headspace of 80% N_2-20% CO_2. Since CO is toxic, it was added to the headspace in small increments (see Materials and Methods). Before each CO addition, the headspace was analyzed to ensure that the CO was fully consumed. As shown in Fig. 4, there was a slow increase in growth as measured by the OD_{600}, but growth did not increase beyond an OD_{600} of 0.2 (one doubling). At this final OD_{600}, added CO was no longer consumed. In the absence of CO addition, there was no increase in yield, confirming that growth did not result from nutrients carried over with the inoculum. A similarly low growth yield on CO was also observed for strain JW3034, with a transposon insertion into the *cooL* subunit gene of the Coo hydrogenase (30). Strain JW9009, lacking *cooA*, showed no increase in OD_{600} or consumption of the initial CO added to the headspace.

The *cooA* deletion can be complemented. We cloned the *cooA* gene and a 270-bp upstream sequence that included the natural promoter into an *E. coli-D. vulgaris* shuttle vector (pMO719) and transformed JW9009 cells to generate strain JW9009(pMO719::*cooA*) (Fig. 5A). To determine if the *cooA* deletion could be complemented by pMO719::*cooA*, we grew JW9009(pMO719::*cooA*)

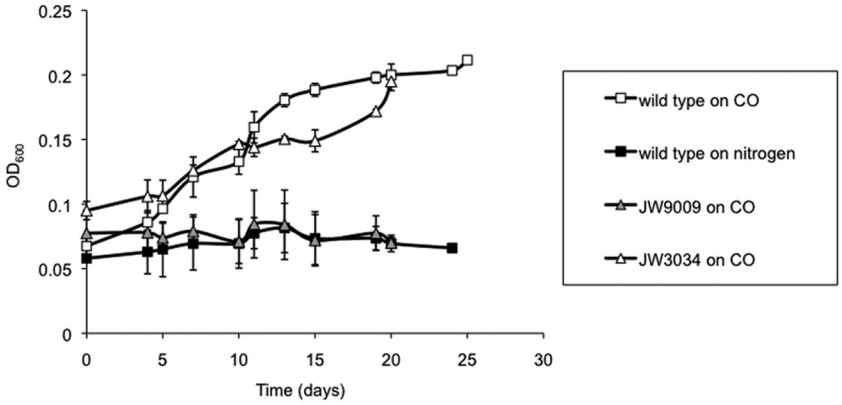

FIG 4 Growth on CO as the sole source of energy. Growth curves (OD_{600}) are shown for the wild type, JW3034, and JW9009 on CO, acetate, and sulfate, with CO added on the following days: for the wild type, 0.7 ml on days 0 and 4, 1 ml on days 5 and 7, 1.2 ml on day 10, 1.5 ml on days 13, 15, 19, and 20, and 1.5 (wt1), 2.0 (wt2), and 2.5 (wt3) ml on day 21; for JW3034 (Δ*cooL*), 0.7 ml on day 0, 1.0 ml on days 5, 8, 10, and 14, 1.2 ml on days 15 and 16, and 1.5 ml on day 19; and for JW9009 (Δ*cooA*), 0.7 ml on day 0.

in PS and LS with 1% CO in the headspace and analyzed the headspace for CO consumption. As shown in Fig. 5B and C, the complemented strain was able to consume the CO on both media. As a negative control, JW9009 was also transformed with the pMO719 empty vector, and this strain did not remove CO (data not shown). This result confirmed that the inability of JW9009 to consume CO was due to deletion of *cooA*, not to downstream polar effects on the *cooS* gene. We observed that in JW9009(pMO719::*cooA*), the CO was consumed very rapidly compared to the case for the wild type. This higher activity was probably because pMO719 is a multicopy plasmid, with the faster removal of CO resulting from multiple copies of *cooA*. The hydrogen bursts seen in these strains were also lower than those for the wild-type and JW9009 strains and correspond to rapid CO removal. A difference in CO metabolism on PS versus LS was observed at later stages of growth with 1% CO. After the CO was nearly depleted and the cells entered stationary phase, there was a small but reproducible CO burst on LS (Fig. 5B).

Strain JW9009 does not accumulate CO during growth on LS or PS. Based on the hypothesis of a role of CO cycling in energy metabolism, we also examined the CO burst profiles for the wild-type, JW9009, and complemented strains. If CO is produced as an intermediate/electron sink during lactate/pyruvate oxidation, then in the absence of CooA, CO should not be removed and is therefore expected to accumulate. However, the *cooA* mutant did not accumulate any more CO than the wild type (Fig. 6A and B versus Fig. 2B and C). A minor burst of CO (Fig. 6C and D) was observed during late-exponential-phase/stationary-phase growth of the JW9009(pMO719::*cooA*) strain on LS. This burst was much smaller than the hydrogen burst and was not observed on PS.

Expression of *cooS*, but not that of *cooL*, depends on CO and CooA. Reverse transcriptase PCR analysis of the *cooS* (CO dehydrogenase) and *cooL* (Coo hydrogenase small subunit) genes was performed on lactate-sulfate cultures of the wild-type, JW9009 (Δ*cooA*), and JW9009(pMO719::*cooA*) strains before and after the addition of CO to the headspace (Fig. 7). There was very little expression of the *cooS* gene in the wild-type strain in the absence of CO (Fig. 7). Expression of this gene was induced by addition of CO. As a control, we measured the expression of the *rpoH* gene, which was constant in all strains and under all conditions tested. In strain JW9009 (Δ*cooA*), there was a low basal level of expression of the *cooS* gene, similar to that observed for the wild type. How-

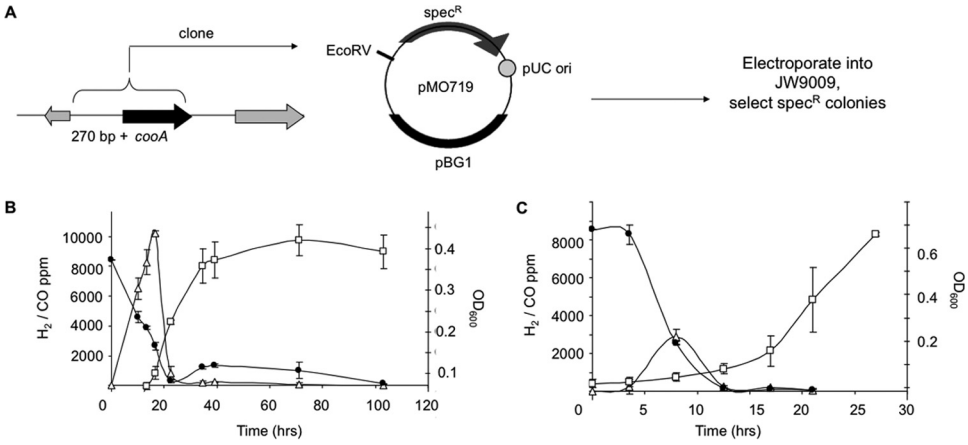

FIG 5 Complementation of *cooA* deletion. (A) Schematic of plasmid complementation. (B and C) Growth (open squares), CO consumption (closed circles), and H_2 (open triangles) profiles for the complemented strain on LS plus 1% CO (B) or PS plus 1% CO (C). Data for panels B and C are for growth in 25-ml Balch tubes with 10 ml medium, with OD_{600} readings measured directly in the Balch tubes. The data are averages for 3 replicates, and error bars show standard deviations.

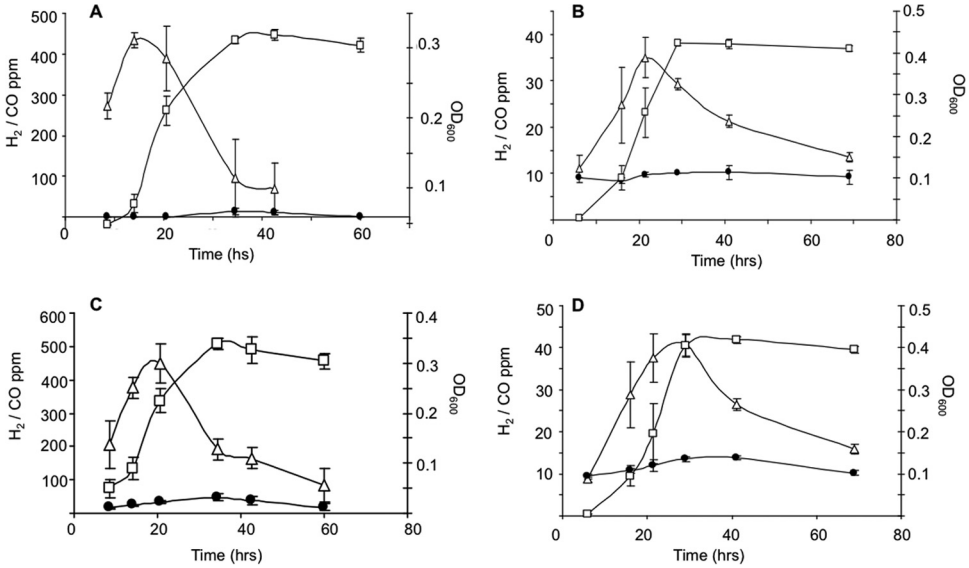

FIG 6 CO and H_2 profiles for JW9009 and the complemented strain. Growth curves (open squares), CO profiles (closed circles), and H_2 profiles (open triangles) are shown for JW9009 in LS (A) and JW9009 in PS (B). (C) Complemented strain on LS; (D) complemented strain on PS. Data are for growth in 250-ml bottles with 100 ml medium, with OD_{600} readings taken by withdrawing 1-ml aliquots into cuvettes.

ever, addition of CO did not change its expression. Interestingly, in the complemented strain JW9009(pMO719::*cooA*), the *cooS* gene seemed to be expressed constitutively. Large amounts of the *cooS* transcript were observed even without CO exposure, and levels did not change after addition of CO.

We also measured transcript levels of the *cooL* gene in all three strains. The *cooL* gene was highly expressed in the wild-type strain. Its expression was not altered by addition of CO, deletion of *cooA*, or the presence of multiple *cooA* copies in the complemented strain (Fig. 7).

Whole-genome transcriptional analysis. Microarray analyses confirmed that exposure of wild-type *D. vulgaris* to CO induced the expression of *cooS* and *cooA* (Table 1; Fig. 8). The most notable effect of CO was a global change in the expression of genes involved in iron homeostasis. A number of genes that are part of the Fur regulon were downregulated, including the ferrous transporter *feoAB* genes (Table 1; Fig. 8). Among the top upregulated genes were membrane protein genes (DVUA0067 and -68) that

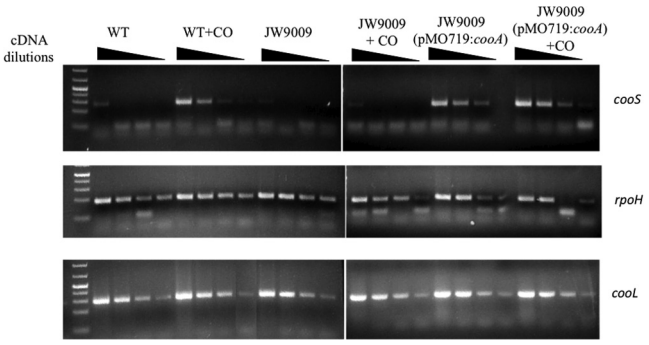

FIG 7 CO and the *cooA* gene are necessary for expression of *cooS*. RT-PCR analysis is shown for the *cooS* and *cooL* transcripts in the WT, JW9009, and complemented strains grown on LS with or without 1% CO. The *rpoH* transcript is shown as an invariant control. Fivefold serial dilutions of cDNA were used for PCR.

are known to be induced by iron (1). DVU0359, a predicted FeS cluster biogenesis protein gene, was one of the most downregulated genes. Together, these changes in expression indicate that in the presence of CO, this organism responds as it would with an excess of ferrous ions. Although the expression of genes in the pathway for sulfate reduction and electron transfer was not significantly affected, the Fe hydrogenase genes (*hydAB* and DVU1769 and -1770) were strongly upregulated. Increased expression of the operon genes DVU3298 to -3302, which encode membrane proteins induced under various stresses (4), and of two putative carbon starvation genes (DVU0598 and -0599) (Table 1; Fig. 8) also points to a possible stress response in the presence of CO.

Deletion of the *cooA* gene resulted in a large number of differentially expressed genes (Table 2), suggesting that CooA serves many regulatory functions even in the absence of exogenous CO. This conclusion is also supported by the downregulation of *cooS* observed in JW9009 relative to the WT, suggesting some expression of these genes in the WT without addition of CO. Focusing on expression changes of at least 2-fold for genes of known function, there were striking parallels in the expression changes induced by deletion of the *cooA* gene and growth of the WT on PS plus CO. These changes included strong upregulation of the Fe-only hydrogenase *hydAB* genes, the iron-induced membrane protein DVUA0067 and -68 genes, and the carbon starvation genes DVU0598 and -99 and significant downregulation of the Fur regulon genes, with a more pronounced effect seen in the mutant strain (Table 1; Fig. 8). The primary differences were increased expression of heme-containing proteins (e.g., cytochrome *c*-related and Hmc proteins) in the *cooA* deletion mutant relative to the WT on PS plus CO and decreased expression of genes coding for the nonheme Rnf electron transfer complex, which is predicted to function as a ferredoxin-NAD^+ oxidoreductase and to mediate an ion motive force (3). Additional changes included reduced expression in strain JW9009 of genes in the operon containing DVU3131 to -34 (coding for a putative sugar-binding tran-

TABLE 1 Key differentially expressed genes in WT and JW9009 strains on pyruvate-sulfate in the presence and absence of CO

Gene category and ID	Gene annotation	WT on PS plus CO vs WT on PS		JW9009 on PS vs WT on PS		JW9009 on PS plus CO vs JW9009 on PS	
		$\log_2 R$ value	Z score[a]	$\log_2 R$ value	Z score[a]	$\log_2 R$ value	Z score[a]
CO utilization genes							
DVU2097	*cooA*	1.926	2.414	−1.021	−1.666	0.262	0.345
DVU2098	*cooS*	2.330	2.379	−1.107	−1.378	0.134	0.209
DVU2099	*cooC2*	0.802	0.964	−0.212	−0.316	0.252	0.362
DVU2286	*cooM*	−0.624	−0.865	0.293	0.484	−0.495	−0.955
DVU2288	*cooL*	−0.537	−0.991	0.326	0.574	−0.478	−0.835
DVU2289	*cooX*	−0.440	−0.789	0.306	0.548	−0.497	−0.946
DVU2290	*cooU*	−0.686	−1.27	0.382	0.708	−0.595	−1.08
DVU2291	*cooH*	−0.516	−0.951	0.216	0.417	−0.414	−0.77
DVU2292	*hypA*	−0.555	−0.784	0.536	0.849	−0.695	−1.32
DVU2293	*cooF*	0.166	0.277	0.562	1.00	−0.601	−1.15
Electron transfer complexes							
DVU0529	*rrf2*	1.461	0.714	2.606	1.577	−1.394	−0.720
DVU0530	*rrf1*	1.477	0.631	3.479	2.338	−1.447	−0.915
DVU0531	*hmcF*	1.263	0.631	2.167	1.061	−0.667	−0.298
DVU0532	*hmcE*	0.473	0.193	2.780	1.469	−1.972	−0.817
DVU0533	*hmcD*	1.283	0.478	3.866	1.793	−1.311	−0.668
DVU0534	*hmcC*	1.886	1.713	1.912	1.609	−0.930	−0.760
DVU0535	*hmcB*	0.988	0.759	0.806	0.537	−0.722	−0.474
DVU0536	*hmcA*	1.280	0.800	1.406	0.781	−0.707	−0.356
DVU2791	Decaheme gene	0.018	0.030	−0.752	−1.114	0.993	1.503
DVU2792	*rnfC*	0.626	0.840	−0.566	−0.764	1.024	1.317
DVU2793	*rnfD*	−0.059	−0.089	−0.656	−0.915	0.860	1.239
DVU2794	*rnfG*	0.116	0.196	−0.726	−1.082	0.979	1.282
DVU2795	*rnfE*	0.484	0.793	0.058	0.064	2.024	2.214
DVU2796	*rnfA*	0.816	1.275	−0.662	−0.989	1.005	1.218
DVU2797	*rnfB*	0.543	0.482	−1.299	−1.417	2.454	2.785
Sulfate reduction genes							
DVU0847	*apsA*	0.565	0.426	1.157	0.872	−0.711	−1.185
DVU0848	*qmoA*	−0.142	−0.159	0.840	0.970	−1.202	−2.135
DVU0849	*qmoB*	0.373	0.314	1.072	0.896	−0.952	−1.756
Fur regulon genes							
DVU2571	*feoB*	−4.022	−1.359	−4.119	−1.630	−0.431	−0.683
DVU2572	*feoA*	−3.694	−2.026	−4.479	−2.149	0.585	0.482
DVU2573	hp gene	−2.296	−1.683	−3.040	−2.120	0.656	0.861
DVU2574	*feoA*	−2.337	−1.952	−2.642	−2.027	0.741	0.884
DVU2680	Flavodoxin gene	−1.794	−1.153	−2.582	−1.549	0.838	1.046
DVU3330	P-type ATPase gene	−1.462	−0.891	−1.929	−1.350	0.443	0.422
DVU3331	Hypothetical protein gene	−0.341	−0.265	−2.196	−1.873	−0.064	−0.080
DVU3332	P-type ATPase gene	−0.110	−0.051	−0.820	−1.097	0.638	0.673
DVU3333	Hypothetical protein gene	−1.897	−1.152	−3.643	−2.447	−0.153	−0.280
DVU0763	GGDEF domain gene	−3.574	−1.425	−1.673	−1.596	0.078	0.119
DVU2378	FoxR regulator gene	−0.762	−0.228	−2.912	−0.886	−0.235	−0.208
DVU2379	Peptidase gene	−1.437	−0.852	−2.349	−1.396	0.801	0.573
DVU2380	ABC transporter gene	−1.434	−0.517	−2.261	−0.863	−0.163	−0.301
DVU2381	Hypothetical protein gene	−1.909	−0.517	−2.742	−0.795	−0.027	−0.026
DVU2382	Conserved domain gene	−0.985	−0.559	−2.639	−1.548	0.558	0.592
DVU2383	TonB receptor gene	−2.890	−0.863	−4.246	−1.324	−0.249	−0.459
DVU2384	ABC transporter gene	−0.597	−0.400	−0.079	−0.087	−0.498	−0.725
DVU2385	ABC transporter gene	0.079	0.094	0.233	0.366	−0.368	−0.610
DVU2386	ABC transporter gene	−0.782	−0.483	−0.281	−0.506	−0.829	−0.978
DVU2387	ABC transporter gene	−0.168	−0.265	0.255	0.394	−0.545	−0.913
DVU2388	TolQ gene	−1.596	−0.850	−1.336	−1.025	−0.011	−0.010
DVU2389	TonB domain gene	−1.640	−1.216	−2.249	−1.902	−0.106	−0.109
DVU2390	TonB domain gene	−1.915	−1.084	−1.438	−1.105	−0.296	−0.348
DVU0303	TPR domain gene	−0.840	−0.554	−2.587	−1.366	1.078	0.821

(Continued on following page)

TABLE 1 (Continued)

Gene category and ID	Gene annotation	WT on PS plus CO vs WT on PS		JW9009 on PS vs WT on PS		JW9009 on PS plus CO vs JW9009 on PS	
		$\log_2 R$ value	Z score[a]	$\log_2 R$ value	Z score[a]	$\log_2 R$ value	Z score[a]
DVU0304	Hypothetical protein gene	−0.284	−0.255	−1.999	−1.477	0.942	0.956
DVU3123	HD domain gene	−0.744	−0.550	−2.011	−2.692	1.237	1.598
DVU3124	Hypothetical protein gene	−0.048	−0.033	−1.905	−1.278	0.598	0.422
DVU0273	Hypothetical protein gene	−2.452	−1.503	−3.189	−1.739	0.837	0.774
Iron-induced genes							
DVU0997	*metF*	−0.484	−0.582	0.955	1.403	−1.138	−1.434
DVU3371	*metE*	−0.147	−0.060	3.161	2.068	−1.251	−0.769
DVUA0067	Membrane protein gene	3.983	1.888	2.702	1.280	0.606	1.094
DVUA0068	Membrane protein gene	5.462	2.008	3.703	1.357	0.594	0.986
Iron-related genes							
DVU0359	HesB domain gene	−3.768	−1.490	−5.608	−2.491	−0.790	−0.950
DVU1769	*hydA*	3.977	2.550	2.686	1.712	0.045	0.072
DVU1770	*hydB*	4.521	2.390	2.864	1.809	0.103	0.149
Cytochrome *c*-related genes							
DVU3107	Cytochrome *c* gene	0.222	0.120	−3.052	−2.793	−0.538	−0.782
DVU1045	Hypothetical protein gene	0.071	0.127	1.327	2.353	−0.624	−1.109
DVU1046	Hypothetical protein gene	0.443	0.609	1.966	2.717	−0.767	−1.440
DVU1047	*ccmC*	−0.797	−0.720	0.779	1.325	−0.818	−1.431
DVU1048	*ccmB*	1.637	0.741	2.623	1.294	−0.848	−1.516
DVU1049	*ccmA*	0.029	0.015	2.559	2.807	−1.633	−3.183
DVU1050	*ccmF*	−0.126	−0.198	1.575	2.561	−1.225	−2.358
DVU1051	*ccmE*	0.048	0.073	0.810	1.457	−0.762	−1.361
DVU1817	Cytochrome *c* 553 gene	−1.041	−1.737	−0.672	−1.074	0.035	0.059
Miscellaneous genes							
DVU3131	Regulator gene	0.026	0.018	−2.607	−1.299	0.565	0.335
DVU3132	G3P dehydrogenase gene	−0.338	−0.231	−1.601	−1.237	0.105	0.089
DVU3133	*glpF* (glycerol uptake gene)	1.170	0.851	−2.889	−1.293	2.892	1.554
DVU3134	*glpK* (glycerol kinase gene)	0.129	0.049	−2.109	−0.863	1.992	1.280
DVU0598	*cstA* carbon starvation gene	3.048	3.604	2.267	2.445	0.505	0.755
DVU0599	*cstA*	3.941	2.778	2.971	1.960	1.004	1.254
DVU3298	Hypothetical protein gene	2.192	1.131	0.480	0.669	1.078	0.457
DVU3299	Hypothetical protein gene	5.362	2.869	2.504	1.345	0.912	0.752
DVU3300	Hypothetical protein gene	6.428	11.291	1.064	0.917	1.270	0.453
DVU3301	Hypothetical protein gene	3.536	4.400	0.918	0.994	0.327	0.187
DVU1141	Hypothetical protein gene	−2.454	−1.420	−3.487	−2.395	1.811	1.620
DVU1142	Regulator gene	−1.914	−0.972	−4.446	−2.963	2.258	2.317
DVU1143	Hypothetical protein gene	0.662	0.708	−1.159	−1.900	0.118	0.185
DVU2805	Vitamin B_{12} biosynthesis gene	−0.231	−0.160	2.309	1.448	0.409	0.279
DVU2806	TolQ family gene	−0.887	−0.542	1.868	2.259	0.439	0.504
DVU2807	Ferric ion uptake family gene	−1.044	−0.393	3.181	1.659	0.553	0.594
DVU1584	*rpoH*	0.555	0.520	0.216	0.203	−0.201	−0.349

[a] Z scores of >1 are considered significant.

scriptional regulator and three proteins annotated as a glycerol-3-phosphate dehydrogenase, a glycerol uptake protein, and a glycerol kinase) and of DVU1141 to -43 (coding for a transcriptional regulator and two hypothetical proteins) (Table 1; Fig. 8). The most parsimonious interpretation of these expression changes is an unknown endogenous source of CO that is sufficient to alter gene expression in the absence of a functional sensor serving to maintain a low basal level of CO. The response to elevated exogenous or endogenous CO may in part be a consequence of the interaction of CO with metalloporphyrins with iron or cobalt centers, which include vitamin B_{12} (24). This could offer an explanation for increased expression of DVU0997 (*metE*), coding for a vitamin B_{12}-independent methionine synthase (Table 1; Fig. 8).

Interestingly, when strain JW9009 was grown on PS plus CO, the most notable changes in transcription (relative to that in JW9009 on PS) were a slight decrease in the expression of genes coding for heme-containing proteins (Hmc, Qmo, and cytochrome *c*-related proteins) and increased expression of genes coding for the nonheme Rnf electron transfer complex (Table 1). No changes were seen in any of the Fur- or iron-regulated genes (Table 1; Fig. 8). In principle, interpretation of JW9009's response to CO is uncomplicated, since the strain cannot remove CO and the

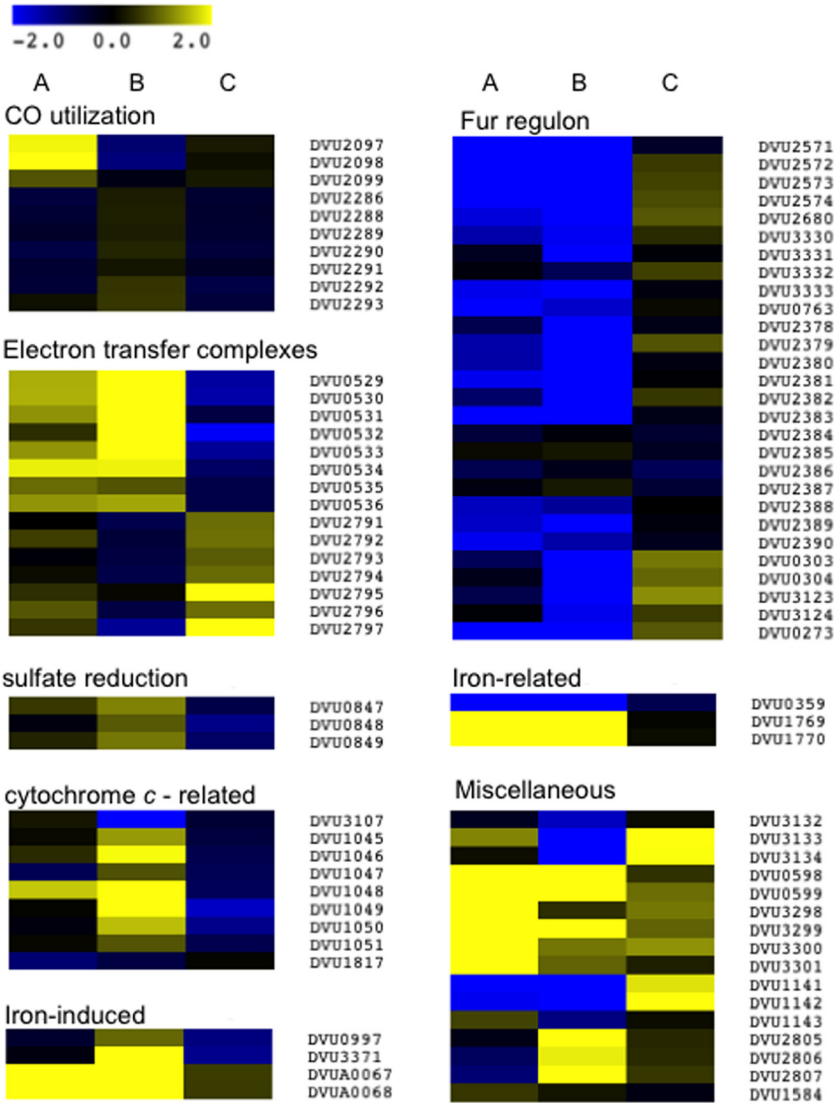

FIG 8 Heat maps of key differentially expressed genes. Global transcriptional changes were measured as $\log_2 R$ ratios for the WT on PS plus CO versus the WT on PS (A), JW9009 on PS versus the WT on PS (B), and JW9009 on PS plus CO versus JW9009 on PS (C). For details, also see Table 1.

growth on PS was not affected by 1% CO. The general comparability of expression patterns of JW9009 grown on PS and PS plus CO again points to a general response to CO, either provided exogenously or produced endogenously.

TABLE 2 Numbers of differentially expressed genes with $\log_2 R$ values of $>|1.0|$ and Z scores of $>|1.0|$

Gene category	No. of genes with $\log_2 R$ values of $>\|1.0\|$ and Z scores of $>\|1.0\|$		
	WT on PS plus CO vs WT on PS	JW9009 on PS vs WT on PS	JW9009 on PS plus CO vs JW9009 on PS
Upregulated genes	224	157	133
Downregulated genes	201	300	47
Total	425	457	180

DISCUSSION

We showed here that *D. vulgaris* Hildenborough has a functional CO dehydrogenase that it uses to efficiently remove exogenous CO from its environment. The strain is also capable of very slow growth using CO as the sole energy source. We showed that DVU2097 (*cooA*) is essential for CO oxidation and that induction of the CODH *cooS* gene in response to CO depends on CooA. This is in contrast to a previous report that failed to detect CO-dependent transcription using heterologously expressed *D. vulgaris* CooA in *E. coli* (32).

Although the *cooMKLUXHF*-encoded hydrogenase of *D. vulgaris* is also homologous to the CO-dependent Coo hydrogenases of *R. rubrum* and *C. hydrogenoformans*, our RT-PCR analysis clearly demonstrated that the expression of the *D. vulgaris* Coo hydrogenase is neither exogenous CO nor CooA dependent. Additionally, the *cooL* mutant also exhibited low growth with CO as the sole energy source, just as the wild type did. Therefore, the

H_2-evolving functions of this hydrogenase (30) are most likely not regulated by any endogenous CO production, and it may be useful to rename this hydrogenase. Which of the remaining five hydrogenases in *D. vulgaris* works with CODH? The second cytoplasm-facing membrane-bound hydrogenase, Ech, is a possibility, but an *ech* transposon mutant was also capable of CO oxidation. It is possible that either the Coo or Ech hydrogenase can function in this role and that a phenotype may be observed only with a double mutant. Alternately, it could be the Fe hydrogenase, as suggested by the upregulation of *hydAB* genes with CO and the overproduction of CO in an *hyd* mutant (29).

Strain JW9009, lacking *cooA*, makes for a useful system to study the effects of exogenous CO on *D. vulgaris*. CO toxicity was seen strongly during growth on lactate-sulfate, where a concentration as low as 1% headspace CO was inhibitory for growth. This effect could be a result of CO inhibition of key uptake hydrogenases such that the resulting elevated H_2 concentrations block further oxidation of lactate. On PS, the pyruvate was fermented at 2% and higher CO concentrations, as seen by the markedly reduced amount of sulfide produced, and this could account for the greater tolerance to CO on PS than on LS. The uptake hydrogenase that is most likely to be affected is the Fe hydrogenase HydAB, since it has the lowest K_i (0.1 μM CO) (2). In support of this hypothesis, expression analysis of the WT strain also showed that the *hydAB* genes were among the most highly induced genes in the presence of CO.

The study also points to a more complex role of CO in the physiology of this organism. Given the extremely poor growth of the WT on CO plus acetate, it is unlikely that CO serves as an environmentally significant growth substrate. Extremely limited growth on CO also suggests that CO cycling, hypothesized to function in concert with H_2 cycling (27), does not offer significant energetic advantages. The lack of a pronounced CO burst in JW9009 is a further indication that CooA does not have a role in CO cycling. This then points to a function in CO detoxification and/or the possible modulation of intracellular concentrations of CO. Studies with a *Desulfovibrio desulfuricans* strain have shown that CO toxicity may be due to oxidative stress resulting from CO oxidation (7, 8). Transcriptomic analysis to study the effects of the CO-releasing molecules CORM-2 and CORM-3 in *E. coli* also suggested the presence of oxidative stress, with Fur regulon genes downregulated with CORM-3 (6) and OxyR and SoxS genes upregulated with CORM-2 (18). CORM-2 was also shown to induce the production of reactive oxygen species in *E. coli* (26). Also, the reduced expression of cytochrome *c* biogenesis genes and the *hmc* genes may reflect a preference for the Rnf complex for electron transfer in the presence of CO, since CO is known to bind strongly to cytochrome *c*. Such stresses could be alleviated by the CODH.

Considering the large number of differentially regulated genes upon deletion of CooA and some expression of *cooS* in the wild type in the absence of CO, our study is also suggestive of a role of endogenously produced CO in cellular signaling. Endogenous CO may be produced by an unknown mechanism from pyruvate oxidation, as suggested previously (29), or by the turnover of enzymes, such as hydrogenases, that use CO as a ligand. Deletion of the CO sensor resulted in both the loss of the ability to consume CO and a significantly altered transcriptional profile on PS that was very similar to that observed for the WT grown on PS plus CO. This result is consistent with a transcriptional response to elevated endogenous CO in the absence of CooA, even though a significant accumulation of CO in the culture headspace was not observed for the *cooA* deletion mutant. *Desulfovibrio* species are rich in metal-containing hydrogenases and proteins implicated in electron transfer reactions. However, as yet, the sites and mechanism of energy conservation remain unresolved. Thus, the indication that CO differentially alters the expression of many genes coding for electron transfer activities provides a significant impetus for additional studies designed to more fully evaluate the functional significance of CO in *Desulfovibrio*.

ACKNOWLEDGMENT

This work, conducted by ENIGMA (Ecosystems and Networks Integrated with Genes and Molecular Assemblies [http://enigma.lbl.gov]), a Scientific Focus Area Program at Lawrence Berkeley National Laboratory, was supported by the Office of Science, Office of Biological and Environmental Research, of the U.S. Department of Energy, under contract no. DE-AC02-05CH11231.

REFERENCES

1. **Bender KS, et al.** 2007. Analysis of a ferric uptake regulator (Fur) mutant of *Desulfovibrio vulgaris* Hildenborough. Appl. Environ. Microbiol. **73**: 5389–5400.
2. **Berlier Y, et al.** 1987. Inhibition studies of three classes of *Desulfovibrio* hydrogenase: application to the further characterization of the multiple hydrogenases found in *Desulfovibrio vulgaris* Hildenborough. Biochem. Biophys. Res. Commun. **146**:147–153.
3. **Biegel E, Schmidt S, Gonzalez JM, Müller V.** 2011. Biochemistry, evolution and physiological function of the Rnf complex, a novel ion-motive electron transport complex in prokaryotes. Cell. Mol. Life Sci. **68**:613–634.
4. **Chhabra SR, et al.** 2006. Global analysis of heat shock response in *Desulfovibrio vulgaris* Hildenborough. J. Bacteriol. **188**:1817–1828.
5. **Cord-Ruwisch R.** 1985. A quick method for the determination of dissolved and precipitated sulfides in cultures of sulfate-reducing bacteria. J. Microbiol. Methods **4**:33–36.
6. **Davidge KS, et al.** 2009. Carbon monoxide-releasing antibacterial molecules target respiration and global transcriptional regulators. J. Biol. Chem. **284**:4516–4524.
7. **Davydova M, Sabirova R, Vylegzhanina N, Tarasova N.** 2004. Carbon monoxide and oxidative stress in *Desulfovibrio desulfuricans* B-1388. J. Biochem. Mol. Toxicol. **18**:87–91.
8. **Davydova MN, Tarasova NB.** 2005. Carbon monoxide inhibits superoxide dismutase and stimulates reactive oxygen species production by *Desulfovibrio desulfuricans* 1388. Anaerobe **11**:335–338.
9. **Fox JD, Kerby RL, Roberts GP, Ludden PW.** 1996. Characterization of the CO-induced, CO-tolerant hydrogenase from *Rhodospirillum rubrum* and the gene encoding the large subunit of the enzyme. J. Bacteriol. **178**: 1515–1524.
10. **He Q, et al.** 2006. Energetic consequences of nitrite stress in *Desulfovibrio vulgaris* Hildenborough, inferred from global transcriptional analysis. Appl. Environ. Microbiol. **72**:4370–4381.
11. **He Y, Shelver D, Kerby RL, Roberts GP.** 1996. Characterization of a CO-responsive transcriptional activator from *Rhodospirillum rubrum.* J. Biol. Chem. **271**:120–123.
12. **Heidelberg JF, et al.** 2004. The genome sequence of the anaerobic, sulfate-reducing bacterium *Desulfovibrio vulgaris* Hildenborough. Nat. Biotechnol. **22**:554–559.
13. **Heo J, Halbleib CM, Ludden PW.** 2001. Redox-dependent activation of CO dehydrogenase from *Rhodospirillum rubrum.* Proc. Natl. Acad. Sci. U. S. A. **98**:7690–7693.
14. **Kerby RL, et al.** 1992. Genetic and physiological characterization of the *Rhodospirillum rubrum* carbon monoxide dehydrogenase system. J. Bacteriol. **174**:5284–5294.
15. **Lupton FS, Conrad R, Zeikus JG.** 1984. Physiological function of hydrogen metabolism during growth of sulfidogenic bacteria on organic substrates. J. Bacteriol. **159**:843–849.
16. **Lupton FS, Conrad R, Zeikus JG.** 1984. CO metabolism of *Desulfovibrio vulgaris* strain Madison: physiological function in the absence or presence of exogenous substrates. FEMS Microbiol. Lett. **23**:263–268.

17. **Mukhopadhyay A, et al.** 2006. Salt stress in *Desulfovibrio vulgaris* Hildenborough: an integrated genomics approach. J. Bacteriol. **188**:4068–4078.
18. **Nobre LS, Al-Shahrour F, Dopazo J, Saraiva LM.** 2009. Exploring the antimicrobial action of a carbon monoxide-releasing compound through whole genome transcription profiling of *Escherichia coli.* Microbiology **155**:813–824.
19. **Noguera DR, Brusseau GA, Rittmann BE, Stahl DA.** 1998. A unified model describing the role of hydrogen in the growth of *Desulfovibrio vulgaris* under different environmental conditions. Biotechnol. Bioeng. **59**: 732–746.
20. **Odom JP, Jr, et al.** 1981. Hydrogen cycling as a general mechanism for energy coupling in the sulfate reducing bacteria, *Desulfovibrio* sp. FEMS Microbiol. Lett. **12**:47–50.
21. **Parshina SN, et al.** 2010. Carbon monoxide as an electron donor for the biological reduction of sulphate. Int. J. Microbiol. **2010**:319527.
22. **Rabus R, Hansen T, Widdel F.** 2006. Dissimilatory sulfate- and sulfur-reducing prokaryotes, p 659–768. *In* Dwarkin M, Falkow S, Rosenberg E, Schleifer K-H, Stackbrandt E (ed), The prokaryotes. Springer, New York, NY.
23. **Rodionov DA, Dubchak I, Arkin A, Alm E, Gelfand MS.** 2004. Reconstruction of regulatory and metabolic pathways in metal-reducing delta-proteobacteria. Genome Biol. **5**:R90.
24. **Seufert K, et al.** 2011. Cis-dicarbonyl binding at cobalt and iron porphyrins with saddle-shape conformation. Nat. Chem. **3**:114–119.
25. **Shelver D, Kerby RL, He Y, Roberts GP.** 1997. CooA, a CO-sensing transcription factor from *Rhodospirillum rubrum*, is a CO-binding heme protein. Proc. Natl. Acad. Sci. U. S. A. **94**:11216–11220.
26. **Tavares AF, et al.** 2011. Reactive oxygen species mediate bactericidal killing elicited by carbon monoxide-releasing molecules. J. Biol. Chem. **286**:26708–26717.
27. **Thompson DK, et al.** 2002. Transcriptional and proteomic analysis of a ferric uptake regulator (fur) mutant of *Shewanella oneidensis*: possible involvement of fur in energy metabolism, transcriptional regulation, and oxidative stress. Appl. Environ. Microbiol. **68**:881–892.
28. **Tsuji K, Yagi T.** 1980. Significance of hydrogen burst from growing cultures of *Desulfovibrio vulgaris* Miyazaki, and the role of hydrogenase and cytochrome c in energy production system. Arch. Microbiol. **125**: 35–42.
29. **Voordouw G.** 2002. Carbon monoxide cycling by *Desulfovibrio vulgaris* Hildenborough. J. Bacteriol. **184**:5903–5911.
30. **Walker CB, et al.** 2009. The electron transfer system of syntrophically grown *Desulfovibrio vulgaris.* J. Bacteriol. **191**:5793–5801.
31. **Wu M, et al.** 2005. Life in hot carbon monoxide: the complete genome sequence of *Carboxydothermus hydrogenoformans* Z-2901. PLoS Genet. **1**:e65. doi:10.1371/journal.pgen.0010065.
32. **Youn H, Kerby RL, Conrad M, Roberts GP.** 2004. Functionally critical elements of CooA-related CO sensors. J. Bacteriol. **186**:1320–1329.
33. **Zane GM, Yen HC, Wall JD.** 2010. Effect of the deletion of qmoABC and the promoter distal gene encoding a hypothetical protein on sulfate reduction in *Desulfovibrio vulgaris* Hildenborough. Appl. Environ. Microbiol. **76**:5500–5509.
34. **Zhou A, et al.** 2010. Hydrogen peroxide-induced oxidative stress responses in *Desulfovibrio vulgaris* Hildenborough. Environ. Microbiol. **12**: 2645–2657.